

MEASUREMENTS OF THE SLAC INJECTOR EMITTANCE*

Roger H. Miller
Stanford University, Stanford, California

Introduction

The six-dimensional volume in phase space enclosing the beam from the SLAC injector has been measured. The design of the injector and preliminary measurements on the prototype injector were reported at the National Particle Accelerator Conference, March 10-12, 1965.¹ This paper reports on similar measurements on the completed injector as installed on the SLAC two-mile accelerator. The measurement methods reported here for both transverse and longitudinal phase volumes differ significantly from those used on the prototype injector. The transverse phase space measurement on the prototype used the two-slit method described by van Steenberg.² The method reported here used a variable aperture plus a glass plate (equivalent to a photographic film). The aperture was large, i.e., it measured the current within a given radius, rather than being a differential element. The two methods and the experimental results are compared. The bunching measurement used on the prototype utilized an rf sweeper operating at the accelerator frequency, while the measurement reported on here was done by adjusting an accelerator section to 90° out of phase and thus introducing an energy spread proportional to the bunch length.

The transverse phase volume was found to be $\sim 5 \times 10^{-4} (\text{m}_{0c}\text{-cm})^2$, the bunch length $\sim 5^\circ$, and the longitudinal momentum spread $\sim 1 \text{ m}_{0c}$ so that the beam is contained in a six-dimensional volume in phase space

$$V_6 \sim 7 \times 10^{-5} (\text{m}_{0c}\text{-cm})^3.$$

Transverse Emittance Volume

The method used to measure the transverse phase volume (Fig. 1) begins by focusing the beam to a minimum spot on a glass slide at beam analyzing station No. 1 (hereafter called BAS 1). Several different collimator apertures are then inserted at the end of the injector; the beam profile was recorded on a glass slide and the fraction of the injector current reaching the slide was measured for each different collimator aperture. The injector current was measured with a toroidal current transformer (BIMO) in front of the collimator. The current reaching the glass slide was measured with an identical toroid at BAS 1. The four-volume occupied by a particular fraction of the injector beam was calculated using the formula:

$$V(r_1, r_2) = \left(\frac{\pi r_1 r_2 \gamma_1}{L_1 \ln \frac{\gamma_2}{\gamma_1}} \right)^2 = \left(\frac{\pi r_1 r_2 \alpha}{\lambda \ln \frac{\gamma_2}{\gamma_1}} \right)^2$$

* Work supported by the U. S. Atomic Energy Commission.

(Presented at 1966 Linear Accelerator Conference, Los Alamos, October 1966)

where

α = average energy gain per wavelength in units of rest energy

γ_1 = injector energy (in units of mc^2)

γ_2 = energy at BAS 1

L_1 = distance which would be required to reach injector energy γ_1 , with the field strength in the accelerator between injector and BAS 1

r_1 = radius of collimator aperture

r_2 = radius at the glass slide within which a fraction f_2 of current falls

The fraction of the injector current contained in this volume is:

$$f = f_1 f_2$$

where f_1 = the fraction of the injector current which passes through the collimator and reaches the slide.

The phase volumes containing 80% of the injector current were found to be 4.8, 5.6, and $10 \times 10^{-4} (\text{m}_{0c}\text{-cm})^2$ for injector currents of 13 mA, 153 mA, and 316 mA, respectively.

Theory of Transverse Emittance Measurement

The radial equation of motion for relativistic particles, ignoring terms of $\frac{1}{\gamma^2}$ and higher, is:

$$x_2 = x_1 + \int_{L_1}^{L_2} p_x \frac{dz}{p_z}$$

Inserting $p_z = \frac{Qz}{\lambda}$, one obtains

$$x_2 = x_1 + \frac{p_x \lambda}{\alpha} \int_{L_1}^{L_2} \frac{dz}{z}$$

where λ is the wavelength of the accelerating rf power.

By integrating, we obtain

$$x_2 = x_1 + \frac{p_x \lambda}{\alpha} \ln \frac{\gamma_2}{\gamma_1} = x_1 + L_1 \theta_1 \ln \frac{\gamma_2}{\gamma_1}$$

or

$$\theta_1 = \frac{\Delta x}{L_1 \ln \frac{\gamma_2}{\gamma_1}}$$

The same equation holds in the y plane, so one finds that the equation for the increment of solid angle is

$$d\Omega = \frac{dx dy}{\left(L_1 \ln \frac{\gamma_2}{\gamma_1}\right)^2} = \frac{dA}{\left(L_1 \ln \frac{\gamma_2}{\gamma_1}\right)^2}$$

The admittance of two circular apertures at L_1 and L_2 is (see Fig. 2):

$$\begin{aligned} V &= \int dA_1 \int dp_x dp_y \\ &= \int dA_1 \int \gamma_1^2 d\Omega \\ &= \left(\frac{\gamma_1}{L_1 \ln \frac{\gamma_2}{\gamma_1}}\right)^2 \int dA_1 \int dA_2 \\ &= \left(\frac{\pi r_1 r_2 \gamma_1}{L_1 \ln \frac{\gamma_2}{\gamma_1}}\right)^2 \end{aligned}$$

Since $\gamma_1 = \alpha \frac{L_1}{\lambda}$, this can be written

$$V = \left(\frac{\pi r_1 r_2 d}{\lambda \ln \frac{\gamma_2}{\gamma_1}}\right)^2$$

There are two noteworthy facts about this formula: (1) The volume is the same if one considers the first aperture to define the displacement intercept dx, dy, and the second the transverse momentum dp_x , dp_y , or vice versa.

(2) The volume calculated is that of a four-dimensional cylinder (not a four-ellipsoid); i.e., the intercepts with the x, p_x plane and y, p_y plane are parallelograms. In general, the surfaces of constant density in phase-space will approximate a four-ellipsoid whose volume is

$$\begin{aligned} V_1 &= \frac{\pi^2 r^2 p_r^2}{2} \\ &= \frac{1}{2} \left(\frac{\pi r_1 r_2}{\lambda \ln \frac{\gamma_2}{\gamma_1}}\right)^2 \end{aligned}$$

However, since for any real beam there will be particles in the region between the four-cylinder defined by the apertures and the inscribed ellipsoid surface of constant density, the volume of the four-cylinder is the proper one to use.

Experiment

As stated above, the beam was focused to a minimum spot on a glass slide at BAS 1. Exposures were taken for several different collimator apertures with all other parameters unchanged. The density of the spots were measured using a

Joyce-Loebl MK III-C microdensitometer with a spacial resolution of about 0.1 millimeters. Figures 3, 4, and 5 are the densities measured with the microdensitometer for injector currents 13.2 mA, 153 mA, and 316 mA, respectively, and with a 0.2-inch collimator inserted. Two density profiles were measured: one horizontal and one vertical intersecting at the maximum density point. At each current, slides were exposed with four collimator apertures, 0.150-inch, 0.200-inch, 0.250-inch, 0.300-inch, but at 153 mA only two of the exposures were usable because of a double exposure. The current profiles obtained from the microdensitometer were analyzed as follows: (1) the horizontal and vertical widths Δx and Δy were measured for densities from 1% to 95% of maximum density in approximately 10% steps; (2) a mean radius $r_2 = \sqrt{\Delta x \Delta y}/4$ for each density was calculated; (3) the current density was multiplied by the mean radius to find

$$\frac{dI}{dr_2} = r_2 J(r_2)$$

and this was plotted against r_2 ; (4) the curve dI/dr_2 was graphically integrated to find $I(r_2)$. This process is illustrated in Fig. 6 for an injector current of 316 mA and a collimator of 0.300-inch. The current $I(r_2)$ was multiplied by the fraction of injector current which passed through the collimator of radius r_1 and this product was plotted against four-volume in phase space.

$$V_4 = \left(\frac{\pi r_1 r_2 \alpha}{\lambda \ln \frac{\gamma_2}{\gamma_1}}\right)^2$$

The above process was repeated for several collimator apertures at each current, and the envelope $I_{\max}(r_1 r_2)$ of the curves was drawn as shown in Fig. 7. Taking the envelope of these curves is equivalent to integrating out to surfaces of constant density and thereby maximizing the population in a given volume of phase space.

The experimental results are summarized in Fig. 8. For currents of 13.2 and 153 mA, 80% of the current was contained in about 5×10^{-4} ($m_0 c$ -cm)². At 316 mA the phase volumes are approximately twice as large as the volumes at 153 mA, which indicates that the density in phase space remained constant as the current was increased above 150 mA. This result may be an accident of the particular adjustment of the injector.

In Appendix A, it is shown that for the cylindrically symmetrical beam having a gaussian distribution in x, y, p_x , and p_y , the results of the aperture plus glass slide method can be compared to the two-slit method by taking the square root of the normalized current and the square root of the four-volume in phase space. Thus for 13.2 mA and 153 mA, approximately 90% of the current would be projected into an area of 2.2×10^{-2} $m_0 c$ -cm in the x- p_x plane. The measurement on the test injector indicated that 90% of the current

was contained within 1.15 m_0c -cm in the x-p_x plane. The factor of 2 disagreement is not understood.

Hopefully the phase volume of beam will be substantially conserved from the injector to the beam switchyard, although there are a number of effects which can increase it. Transverse forces due to the rf fields, such as those resulting from coupler asymmetries, increase the transverse phase volume of the beam. Lens aberrations, while not actually increasing the volume, distort it so that for practical purposes the volume is increased. Assuming that these effects are not too important, the injector phase volume determines the minimum spot achievable in the end station if the aperture of the last lens and the distance to the focus are fixed. Thus

$$r_2 = \frac{LV^{\frac{1}{2}}}{\pi r_1 \gamma}$$

where

- r_2 = radius of the beam at the beam waist
- r_1 = radius of the beam at the lens
- L = distance from the lens to the beam waist
- V = transverse emittance of the accelerator

Longitudinal Phase Space

The bunch length and momentum spread of the beam from the injector was measured using the momentum spectrometer shown in Fig. 1, which is located after the fourth 3-meter accelerating section. The bunch measurement was accomplished by adjusting the phase of one (or more) of the 3-meter accelerating sections so that it added no energy to the beam, i.e., was 90° out of phase with the bunches. This introduces a known linear correlation between energy and phase, so that a measurement of the energy spectrum is equivalent to a measurement of bunch length. This method was described by Neal in 1953.⁴

If two spectra are taken, one with the analyzing 3-meter section 90° ahead of the bunch, and one with the analyzing section 90° behind, it is possible to avoid errors due to any linear correlation between energy and phase in the beam from the injector. Thus, if E^+ and E^- are the energies of the beam with the analyzing ahead 90° and behind 90°, respectively,

$$E^+(\theta) = E_0(\theta) + E_1 \cos(\phi_1 + \theta) + E_2 \cos(\phi_2 + \theta)$$

$$E^-(\theta) = E_0(\theta) + E_1 \cos(\phi_1 + \theta) + E_2 \cos(-\phi_2 + \theta)$$

where

θ = phase of electron relative to some reference phase, for example the middle of the bunch

$E_0(\theta)$ = energy modulation produced in the bunching process within the injector

- E_1 = maximum energy gain in the injector 3-meter accelerator section
- ϕ_1 = average phase of bunch in injector
- E_2 = maximum energy gain in analyzing section
- ϕ_2 = phase in analyzing section

The differentials of the energy are

$$\delta E^+(\theta) = \left[\frac{dE_0}{d\theta}(\theta) - E_1 \sin(\phi_1 + \theta) - E_2 \sin(\phi_2 + \theta) \right] \delta \theta$$

$$\delta E^-(\theta) = \left[\frac{dE_0}{d\theta}(\theta) - E_1 \sin(\phi_1 + \theta) - E_2 \sin(-\phi_2 + \theta) \right] \delta \theta$$

Combining δE^+ and δE^- one finds

$$\delta \theta = \frac{\delta E^- - \delta E^+}{2E_2 \sin \phi_2 \cos \theta}$$

or for θ small and $\phi_2 = 90^\circ$

$$\delta \theta = \frac{\delta E^- - \delta E^+}{2E_2}$$

Thus the bunch width can be found by taking the average of the spectrum widths with the analyzing section at +90° and at -90° and dividing by the energy contribution of the analyzing section. Averaging the two measurements removes the effect of any linear correlation between energy and phase in the beam from the injector. Figure 9 presents a sample of the bunching data, with spectra for the injector alone, and for the injector plus the analyzing section at 0°, +90°, and -90°.

The bunch shown here is 3° full width at half maximum, 4° wide at 1/3 maximum, and 7° wide at 1/10 maximum. This measurement technique becomes difficult at moderately high currents because of beam loading energy transients. Such a case is shown in Fig. 10. Here the injector and the next 3-meter section were kept in phase and the following two sections, which together contributed 82.5 MeV, were phased to 0° (not shown), +90° and -90°. In this case, taking spectra at both +90° and -90° enables the experimenter to see both halves of the bunch unobscured by the beam loading energy transient on the high energy side of the spectra. The structure on the high energy side cannot be bunch structure since it remains on the high energy side for both the +90° and the -90° spectra, rather than having mirror symmetry. This bunch is 5° wide at 1/2 maximum, 6° wide at 1/3 maximum, and 8° wide at 1/10 maximum. It is interesting to note that the beam loading transient shows considerable fine structure not predicted by simple theory, but presumably due to the dispersion effects described by Leiss.⁵

The bunch widths measured range from 3° to 7°, full width at half maximum, 4° to 8° at 1/3 maximum, and 7° to 13° at 1/10 of maximum. It should be pointed out that this measurement includes the effect of phase modulation (within the pulse and pulse-to-pulse) of the rf from the in-

jector klystron relative to the rf from the klystron driving the analyzing section. This explains the larger bunches reported here compared with the measurement of bunch length of 2.7° full width at $1/3$ maximum from the prototype buncher reported in Ref. 1. In the previous measurement the bunching was measured using a rf sweeper driven by the same klystron driving the prototype buncher. The phase modulation through each klystron measured approximately 3° .

The momentum spread of the beam typically measures between 0.5 and 0.6 MeV/C full width at half maximum when the injector is run with one other section which is phased so as to minimize the spectrum width as in Fig. 10. This effectively measures the momentum spread at a waist in longitudinal phase space. Assuming a bunch length of 5° , this yields a value of ≈ 0.13 (m_0c -cm) for the area in longitudinal phase space. It is not possible at present to state what fraction of the total current lies within this area because the momentum spectrometer has secondary emission foils whose sensitivity is not known, and beam scattering from the vacuum envelope at about $\pm 10\%$ of center energy makes it impossible to integrate under the broad spectra obtained in the bunch measurement. The area measured is of course the projection of the six-dimensional phase space onto the $z - p_z$ plane. Conversely, in the transverse measurements the six-space is projected onto the transverse four-space. Finally, the product of the two measurements yields

$$V_6 \approx 7 \times 10^{-5} (m_0c\text{-cm})^3.$$

References

1. R. H. Miller, R. F. Koontz, and D. D. Tsang, "The SLAC Injector," IEEE Trans. Nucl. Sci. NS-12 (No. 3), 804 (1965).
2. A. van Steenbergen, "Evaluation of Phase-Space Density Measurement Techniques," BNL Accelerator Dept. Internal Report AADD-92, Brookhaven National Laboratory, Upton, New York (September 1965).
3. A. van Steenbergen, BNL Accelerator Dept. Internal Report AvS-2, Brookhaven National Laboratory, Upton, New York (August 1962).
4. R. B. Neal, "A High Energy Linear Electron Accelerator," ML Report No. 185, Microwave Laboratory, Stanford University, Stanford, California (February 1952); pp. 170-73.
5. J. E. Leiss, "Beam Loading in Linear Accelerators," IEEE Trans., Nucl. Sci. NS-12 (No. 3), 804 (1965).

Appendix A

Comparison of Aperture Plus Glass Plate With Two-Slit Measurement

In this appendix, we will compare the aperture plus glass plate technique used here with the two-slit technique used to measure the optics of the prototype injector.¹ Van Steenbergen² makes similar comparisons but does not include the case of an aperture plus glass plate.

The technique consisted of measuring the current through two slits, Fig. 11, as a function of position x_1 and angle $\theta = x_2 - x_1/L$. This yielded a density in the two-dimensional phase space x, p_x which is a projection of the particles in the four-dimensional phase space onto the $y = p_y = 0$ plane. While it is impossible to state a precise relationship between the results of the two-measurement methods for any arbitrary beam, it is useful to compare the two measurements for an idealized beam having an analytic density distribution in phase space. For example, we shall take the Gaussian distribution

$$\begin{aligned} \frac{\partial^4 I}{\partial x_1 \partial y \partial p_x \partial p_y} &= \frac{1}{\pi^2 a^2 b^2} \exp \left[- \left(\frac{x^2 + y^2}{a^2} + \frac{p_x^2 + p_y^2}{b^2} \right) \right] \\ &= \frac{1}{\pi^2 a^2 b^2} \exp \left(- \frac{r^2}{a^2} + \frac{p_t^2}{b^2} \right) \end{aligned} \quad (A.1)$$

where p_t is the transverse momentum.

The two-slit method measures the integral of this over all y and p_y :

$$\begin{aligned} \frac{\partial^2 I}{\partial x \partial p_x} &= \frac{\exp \left[- \left(\frac{x^2}{a^2} + \frac{p_x^2}{b^2} \right) \right]}{\pi^2 a^2 b^2} \int_{-\infty}^{\infty} \exp \left(- \frac{y^2}{a^2} \right) dy \int_{-\infty}^{\infty} \exp \left(- \frac{p_y^2}{b^2} \right) dy \\ &= \frac{1}{\pi ab} \exp \left[\left(- \frac{x^2}{a^2} + \frac{p_x^2}{b^2} \right) \right] \end{aligned} \quad (A.2)$$

The data from the test injector was analyzed by plotting contours of constant density, i.e.,

$$\frac{x^2}{a^2} + \frac{p_x^2}{b^2} = \frac{K^2}{ab} \quad (A.3)$$

The area inside the contour is:

$$A = \pi K^2, = \pi x_0 p_0 \quad (A.4)$$

where x_0 and p_0 are the intercepts with the $p_x = 0$ and $x = 0$ axes, respectively.

$$dA = 2\pi K dK \quad (A.5)$$

and the current inside the contour is:

$$\begin{aligned} I(K) &= \frac{1}{\pi ab} \int \exp \left(- \frac{K^2}{ab} \right) dA = \frac{2}{\pi ab} \int \exp \left(- \frac{K^2}{ab} \right) K dK \\ I(K) &= \left[1 - \exp \left(- \frac{K^2}{ab} \right) \right] = \left[1 - \exp \left(- \frac{x_0 p_0}{ab} \right) \right] \end{aligned} \quad (A.6)$$

So we find that we have a normalized current $[1 - \exp(K^2/ab)]$ in a phase area πK^2 .

We will now analyze the same distribution using two apertures of radii r_1 and r_2 . The first

step in the experiment was to focus the beam onto the glass slide which is equivalent to the transformation

$$\begin{aligned} x'_1 &= x_1 \\ y'_1 &= y_1 \\ p'_x &= p_x - \frac{\gamma_1 x_1}{L_1 \ln(\gamma_2/\gamma_1)} \\ p'_y &= p_y - \frac{\gamma_1 y_1}{L_1 \ln(\gamma_2/\gamma_1)} \end{aligned} \quad (\text{A.7})$$

Accelerating the beam from $z = L_1$ to $z = L_2$ is equivalent to the transformation:

$$\begin{aligned} x_2 &= x'_1 + \left(\frac{L_1 \ln(\gamma_2/\gamma_1)}{\gamma_1} \right) p'_x = \frac{L_1 \ln(\gamma_2/\gamma_1)}{\gamma_1} p_x \\ y_2 &= y'_1 + \left(\frac{L_1 \ln(\gamma_2/\gamma_1)}{\gamma_1} \right) p'_y = \frac{L_1 \ln(\gamma_2/\gamma_1)}{\gamma_1} p_y \end{aligned} \quad (\text{A.8})$$

so the distribution may be expressed in terms of the position coordinates at the first and second apertures as follows:

$$\begin{aligned} &\frac{\partial^4 I}{\partial x_1 \partial y_1 \partial x_2 \partial y_2} \\ &= \frac{\gamma^2 \exp \left[\left(-\frac{x_1^2 + y_1^2}{a^2} - \frac{\gamma^2 (x_2^2 + y_2^2)}{[bL_1 \ln(\gamma_2/\gamma)]^2} \right) \right]}{[\pi ab L_1 \ln(\gamma_2/\gamma_1)]^2} \end{aligned} \quad (\text{A.9})$$

Converting to polar coordinates and integrating over the two azimuthal angles yields:

$$\frac{\partial^2 I}{\partial r_1 \partial r_2} = \frac{4r_1 r_2}{[abL_1 \ln(\gamma_2/\gamma_1)]^2} \exp \left(-\frac{r_1^2}{a^2} - \frac{\gamma_2 r_2^2}{[bL_1 \ln(\gamma_2/\gamma)]^2} \right) \quad (\text{A.10})$$

The r_1 and r_2 integrals are separable with independent limits of integration since the area element in circle r_1 can illuminate the full circle r_2 . This is equivalent to the statement that the volume in phase space is a four-cylinder.

$$\begin{aligned} I(r_1, r_2) &= \frac{4\gamma^2}{[abL_1 \ln(\gamma_2/\gamma_1)]^2} \int_0^{r_1} r_1 \exp \left(-\frac{r_1^2}{a^2} \right) dr_1 \\ &\cdot \int_0^{r_2} r_2 \exp \left(-\frac{\gamma_2 r_2^2}{[bL_1 \ln(\gamma_2/\gamma_1)]^2} \right) dr_2 \end{aligned} \quad (\text{A.11})$$

$$I(r_1, r_2) = \left[1 - \exp \left(-\frac{r_1^2}{a^2} \right) \right] \left[1 - \exp \left(-\frac{\gamma_2 r_2^2}{[bL_1 \ln(\gamma_2/\gamma_1)]^2} \right) \right] \quad (\text{A.12})$$

The volume we have seen is:

$$V_4 = \left(\frac{\pi r_1 r_2 \gamma_1}{L_1 \ln(\gamma_2/\gamma_1)} \right)^2 \quad (\text{A.13})$$

For a constant volume V_4 , the current is maximized by letting the two exponentials in Eq.(A.12) be equal.

$$\frac{r_1}{a} = \frac{\gamma_1 r_2}{bL_1 \ln(\gamma_2/\gamma_1)} = \frac{r_1 p_t}{ab} \quad (\text{A.14})$$

then

$$I_{\max}(r_1, p_t) = \left[1 - \exp \left(-\frac{r_1 p_t}{ab} \right) \right]^2 \quad (\text{A.15})$$

and

$$V_4 = (\pi r_1 p_t)^2 \quad (\text{A.16})$$

Thus for the Gaussian distribution chosen, the comparison between the two-aperture measurement and the two-slit measurement is made by taking the square root of the current $I_{\max}(r, p)$ and the square root of the phase volume V_4 and comparing them to the current $I(x, p_x)$ and the area $A = (\pi x p_x)$.

List of Figures

1. Experimental setup.
2. Geometry of injector emittance measurement.
3. Injector current profile: $I = 13.2$ mA; $r = 0.254$ cm at glass slide.
4. Injector current profile at glass slide: $I = 153$ mA; $r_1 = 0.254$ cm.
5. Injector current profile at glass slide: $I = 316$ mA; $r_1 = 0.254$ cm.
6. Analysis of beam profiles from glass slides.
7. Normalized current vs 4-volume injector current = 316 mA.
8. Normalized current vs 4-volume in phase space.
9. Bunch measurement data: $I = 5$ mA, bunch length = 3° .
10. High current bunch measurement: $I = 85$ mA.
11. Two-slit emittance measurement.

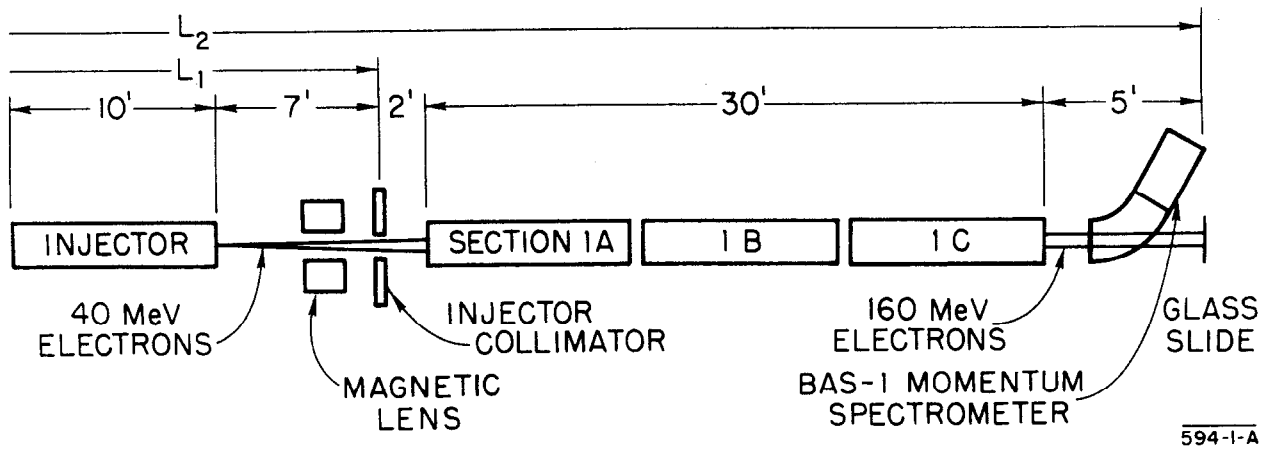
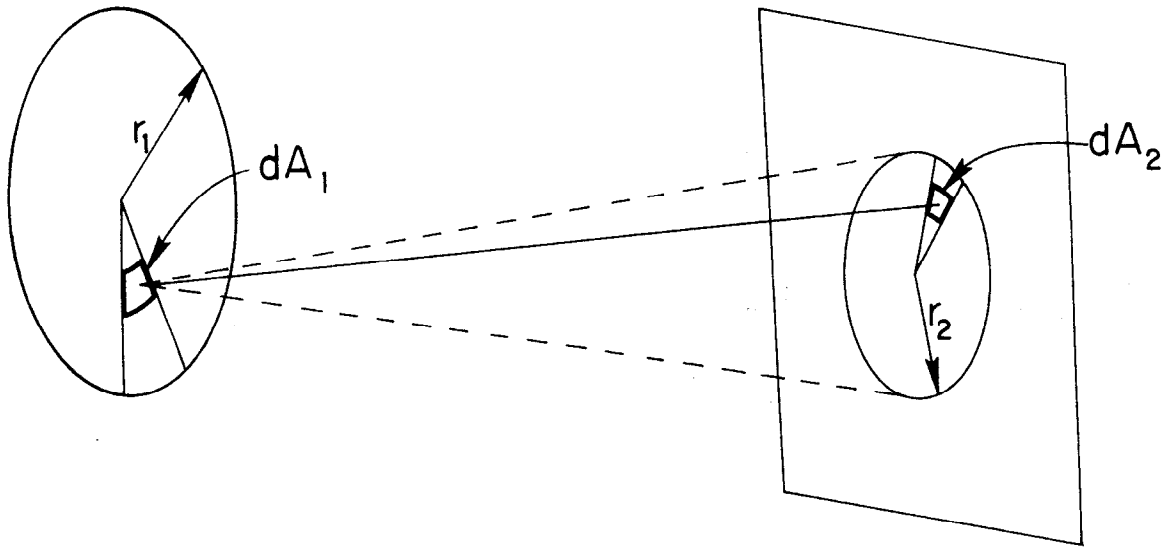
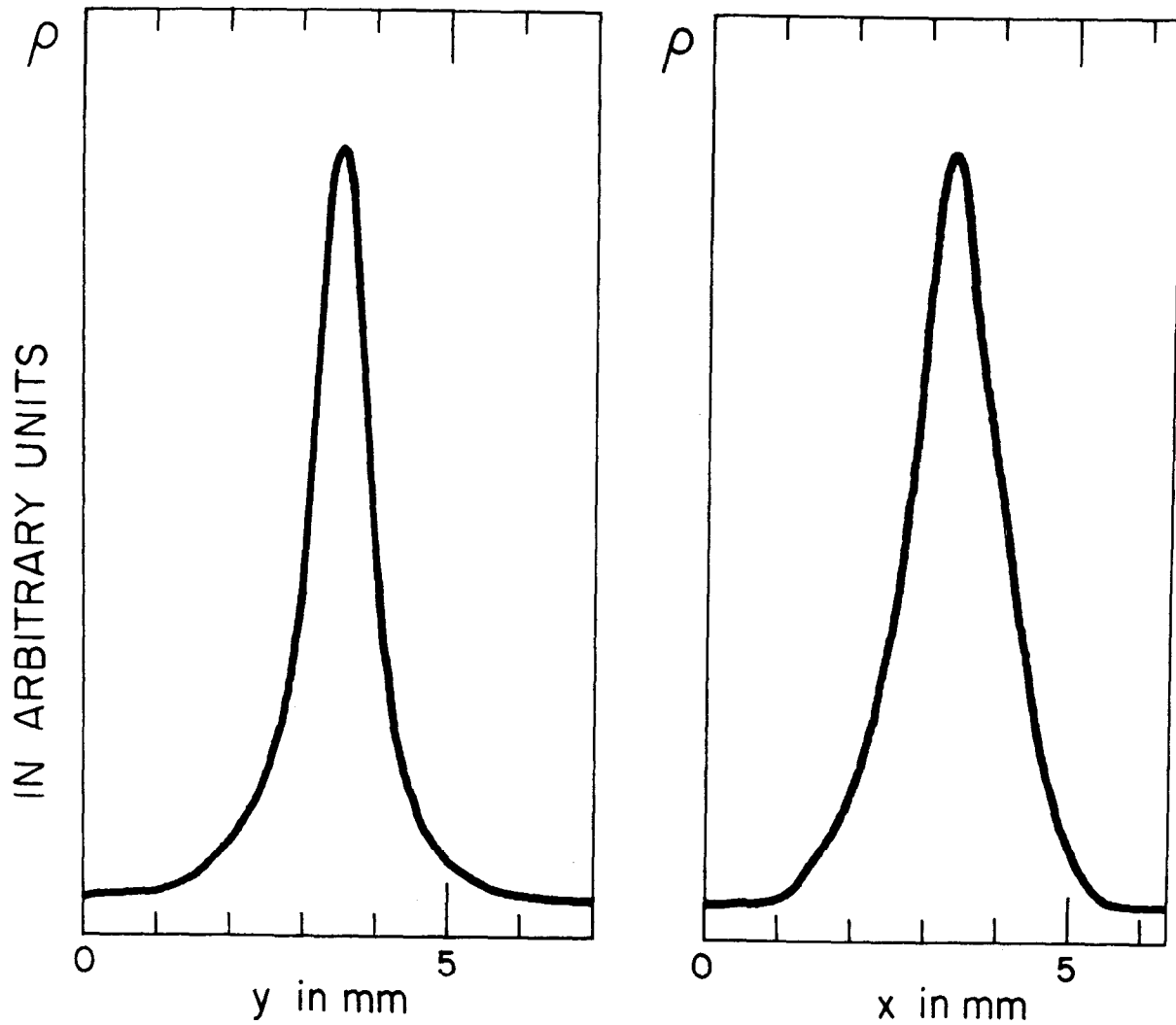


FIGURE 1 -- EXPERIMENTAL SETUP.



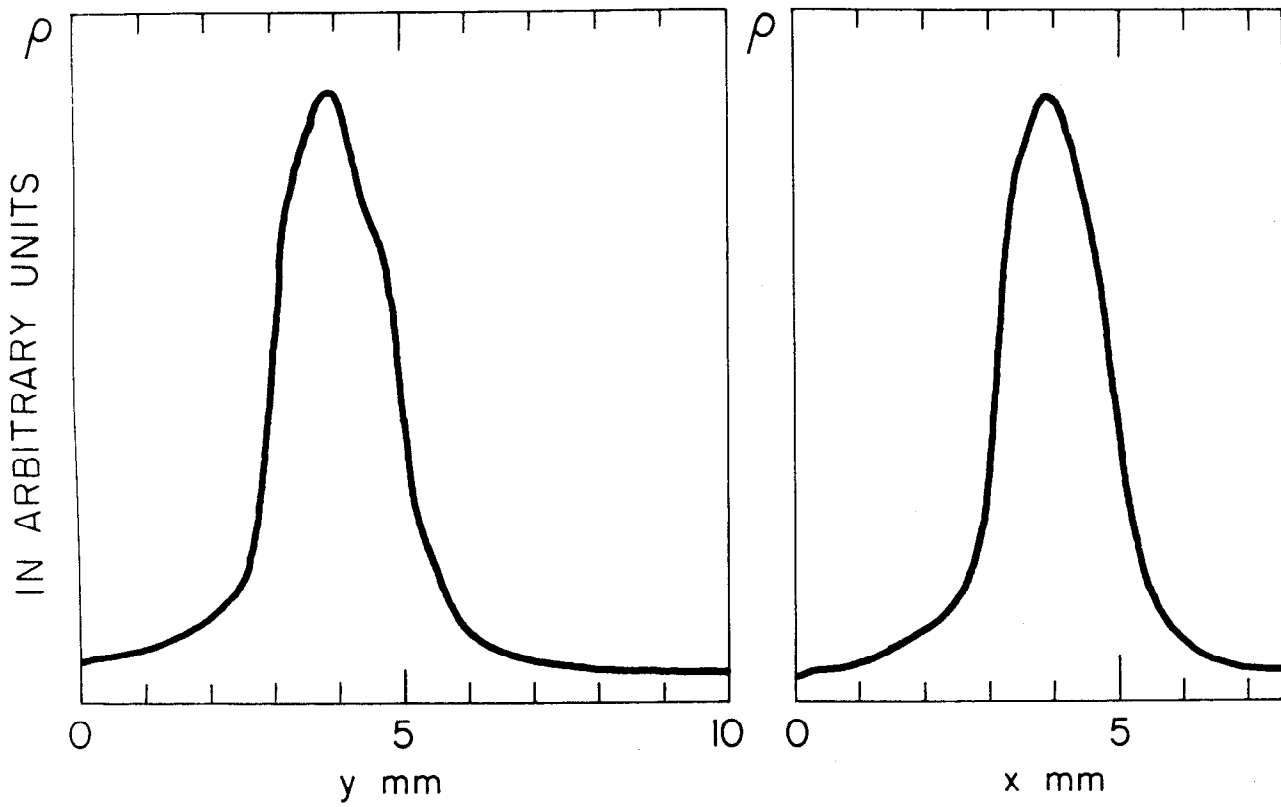
594-2-A

FIGURE 2 -- GEOMETRY OF INJECTOR EMITTANCE MEASUREMENT



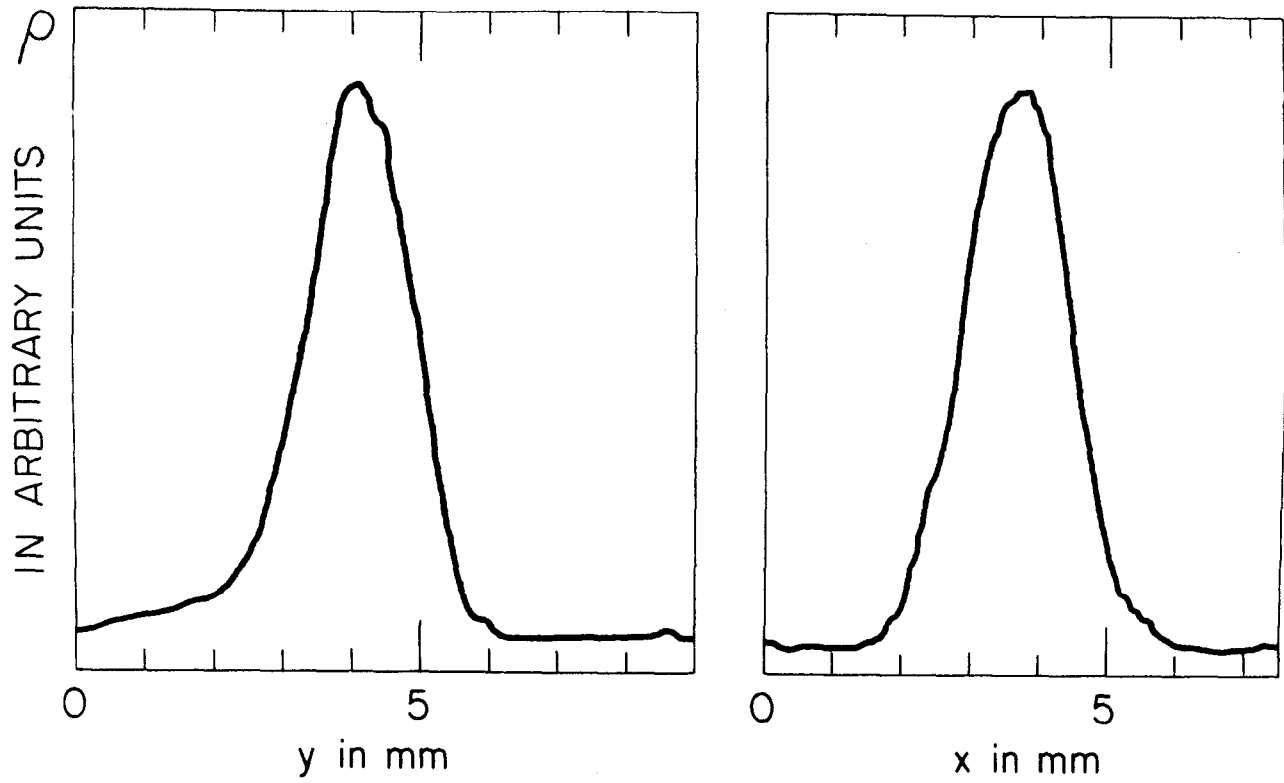
594-3-A

FIGURE 3 -- INJECTOR CURRENT PROFILE; $I=13.2$ mA; $r=0.254$ cm
AT GLASS SLIDE .



594-4-A

FIG. 4 -- INJECTOR CURRENT PROFILE AT GLASS SLIDE
 $I = 153 \text{ mA}$; $r_1 = 0.254 \text{ cm}$.



594-5-A

FIG. 5 -- INJECTOR CURRENT PROFILE AT GLASS SLIDE
 $I = 316 \text{ mA}$, $r_1 = 0.254 \text{ cm}$.

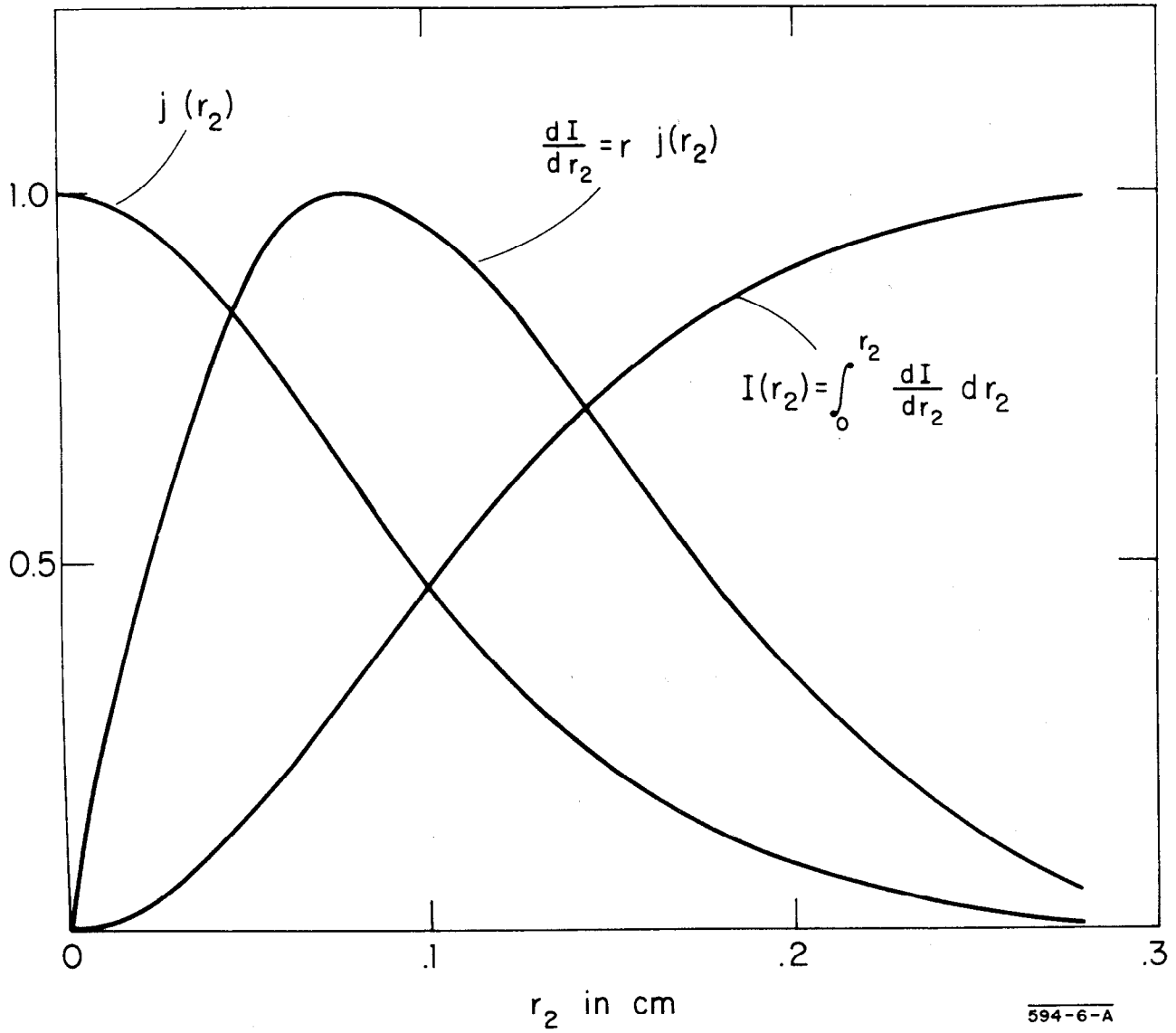


FIG. 6--ANALYSIS OF BEAM PROFILES FROM GLASS SLIDES

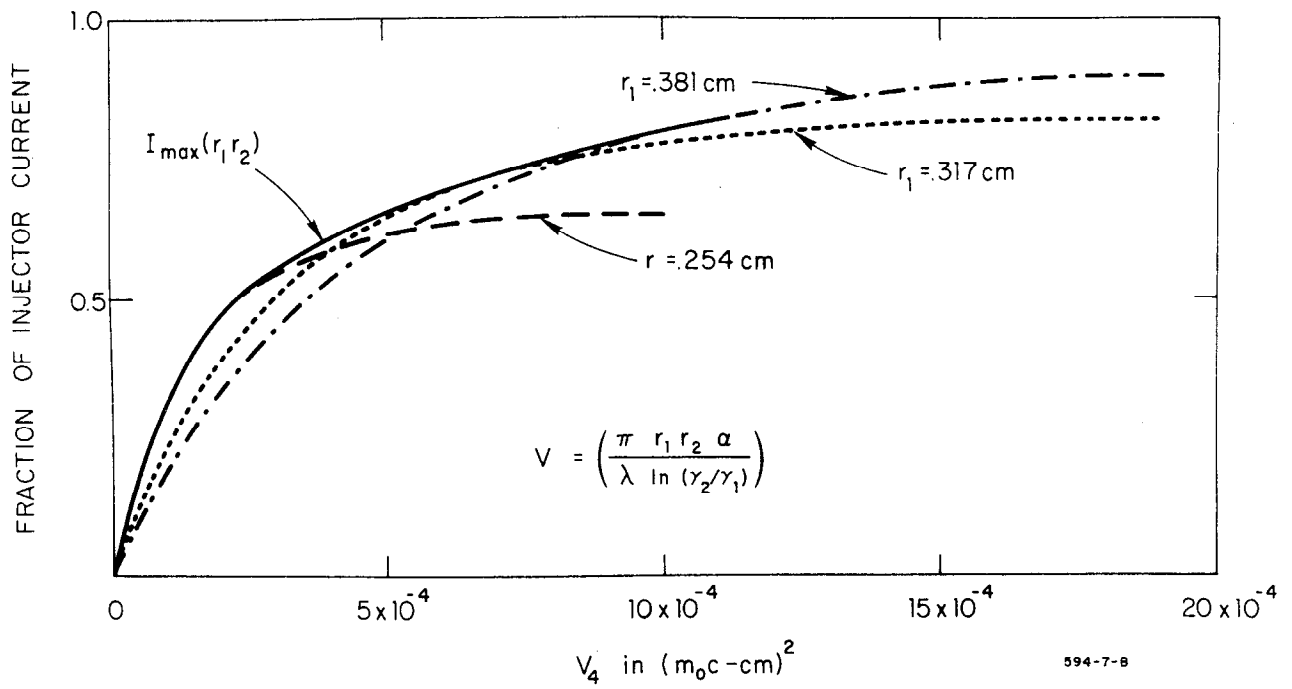


FIG. 7--NORMALIZED CURRENT vs 4-VOLUME INJECTOR CURRENT = 316mA

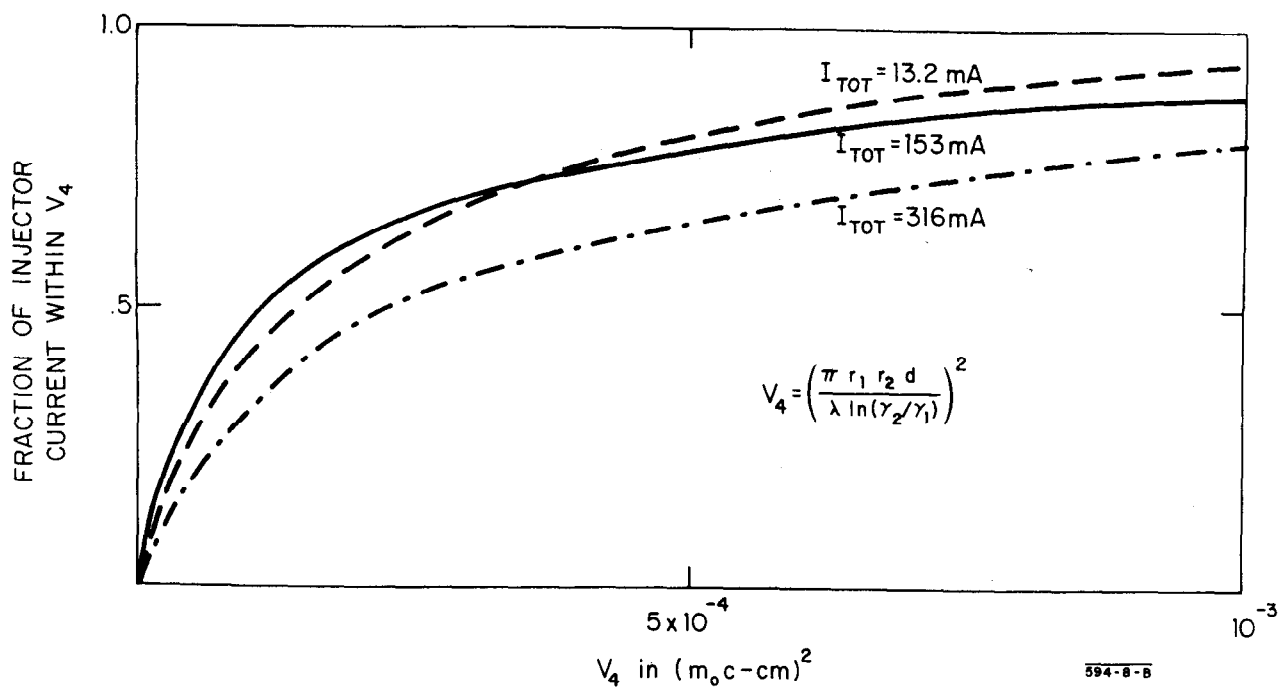


FIG. 8--NORMALIZED CURRENT vs 4-VOLUME IN PHASE SPACE

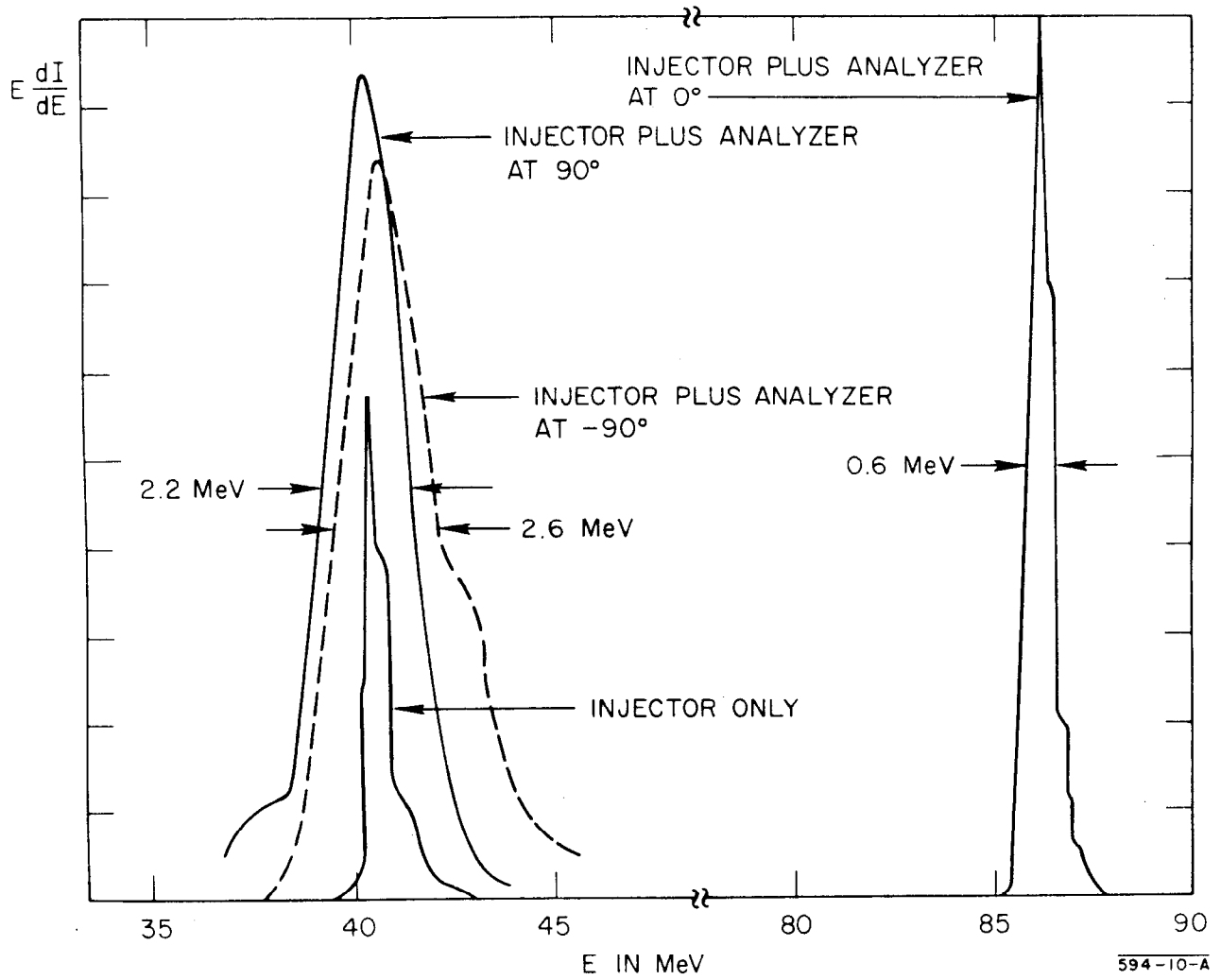


FIG. 9 -- BUNCH MEASUREMENT DATA: $I = 5 \text{ mA}$, BUNCH LENGTH = 3°

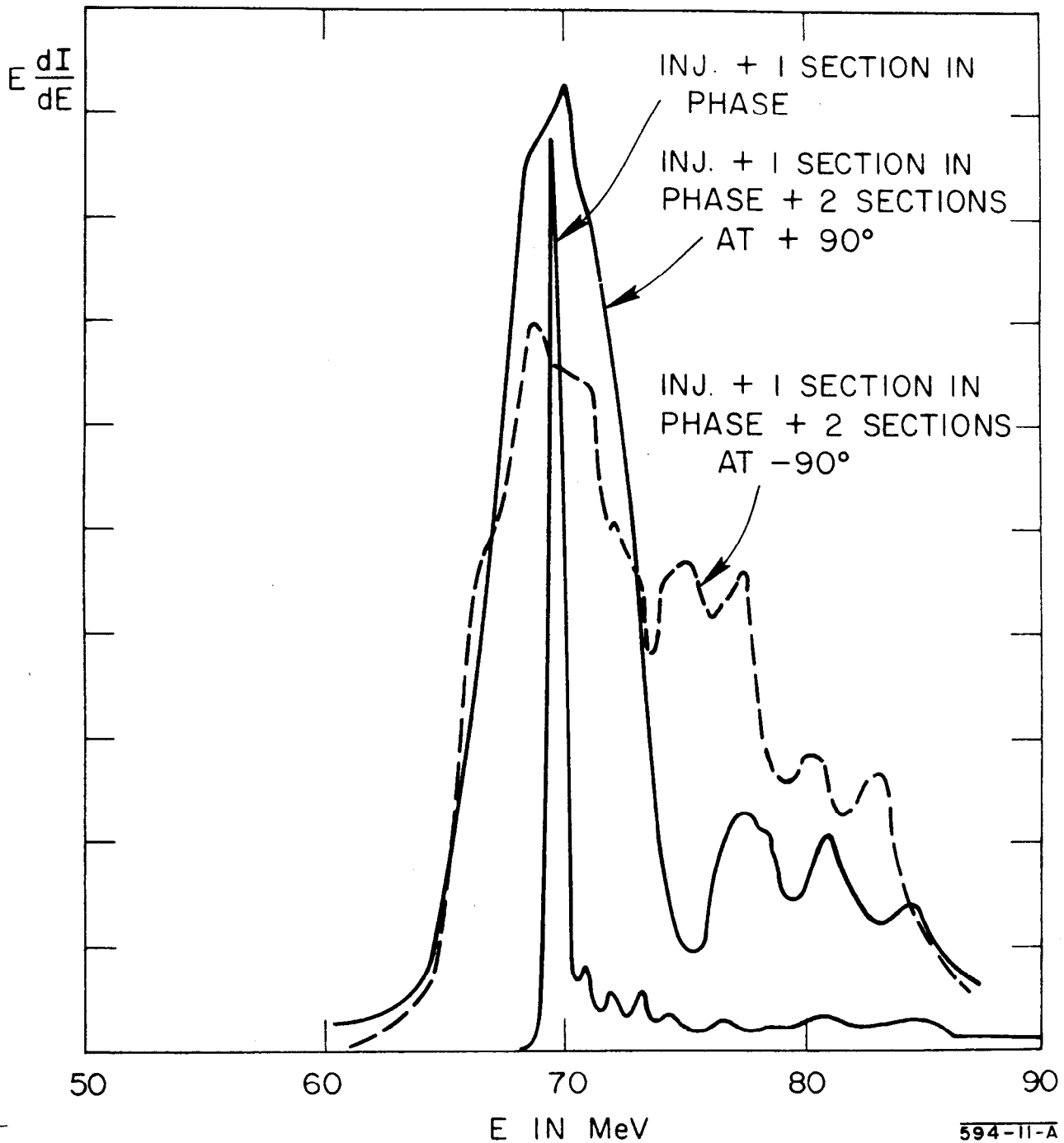


FIG. 10 -- HIGH CURRENT BUNCH MEASUREMENT: $I = 85$ mA

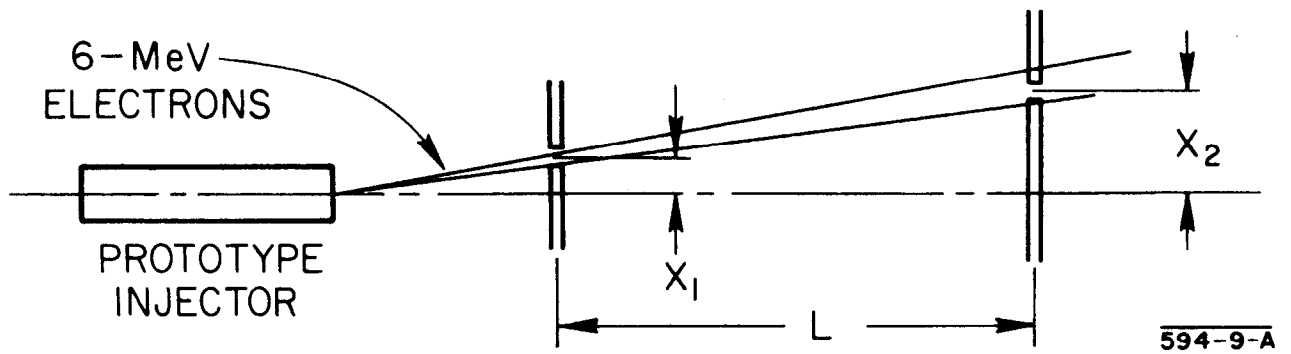


FIG. II -- TWO-SLIT EMITTANCE MEASUREMENT